Scrutiny of the 3-D Non-planar Fault Model of the 1992 Landers Earthquake

Hideo Aochi[1] and Eiichi Fukuyama[2],

(1) Laboratoire de Géologie, École Normale Supérieure, Paris, France (e-mail: aochi@geologie.ens.fr, phone: +33-1 44 32 22 04, fax: +33-1 44 32 22 00). (2) National Research Institute for Earth Science and Disaster Prevention, Tsukuba, Japan (e-mail: fuku@bosai.go.jp, phone: +81-298-51-1611, fax: +81-298-54-0629).

Abstract

Recently, Aochi and Fukuyama (2000, in preparation) proposed the dynamic rupture model of the 1992 Landers earthquake based on a non-planar fault simulation in 3D elastic medium. A simple setting of local tectonics and friction laws could reproduce the qualitative feature of the earthquake, however there still remains uncertainty in the parameters, especially the spatial distribution of frictional parameters. Comparing with the observation and the results of other studies, we discuss the assumption we used and point out its limit of applicability.

Introduction

The boundary integral equation method (BIEM) is a powerful tool for calculating responses of elastic medium and simulating dynamic rupture process (Bonnet, 1995[2]), since we write down the relation between stress field and slip movements on the fault. This method has been widely used for the purpose of understanding rupture physics (e.g. Aki and Richards, 1980[1]). However, since homogeneous and unbounded region in 2D or 3D is commonly assumed, some difficulties are accompanied when it is applied for a realistic earthquake (Quin, 1990[11]). Aochi and Fukuyama (2000, in preparation) applied a 3D-BIEM on the 1992 Landers earthquake considering the non-planar structure of the fault system. Though it was rather easy to demonstrate qualitatively the observed characteristic features such as the rupture transfer between several faults by assuming the fault structure and the background tectonic loading force, there still remains uncertainty about the field information before the earthquake in order to explain the quantitative data such as the surface fault slip and seismograms. Even if a simple planar fault is assumed, the rupture process is very sensitive for the initial condition (Peyrat *et al.*, 2000[10]). Here, we discuss this kind of difficulties based on the numerical model (Aochi and Fukuyama, 2000) for further progresses of earthquake generation physics.

Model

First, we show a fault model in Figure 1. It was constructed based on the surface traces (Hart *et al.*, 1993[5]) and it includes both types of faults which did break in the 1992 rupture and which did not. Thus the model allows rupture to progress spontaneously within potential paths. Next, we consider background tectonic system in order to give the initial stress field before the rupture. Based on the local tectonic setting (Dokka and Travis, 1990[4]; Unruh *et al.*, 1994[15]; Sowers *et al.*, 1994 [14]), we suppose a triaxial compression force gives the
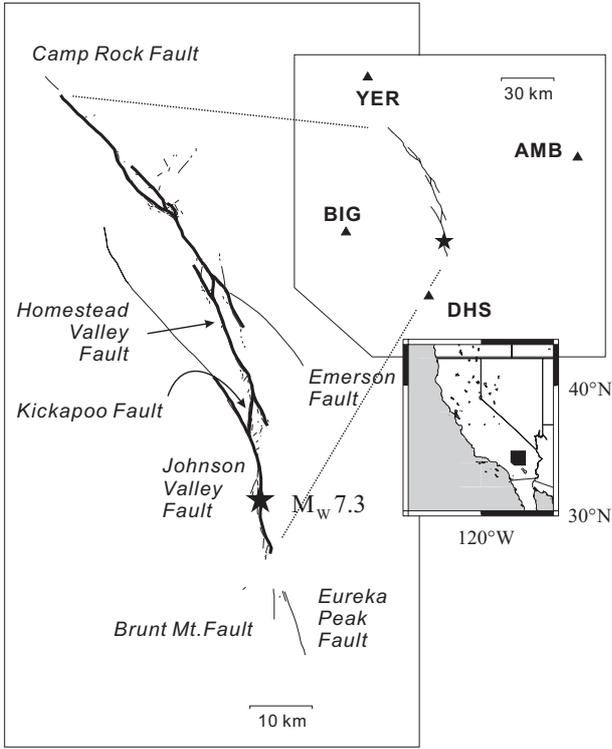
Figure 1: [left] The non-planar fault model (bold line) used in this study and surface traces (thin lines) observed by Hart *et al.* (1993). The star and the triangles express the epicenter and the observation points, respectively. Strong motion stations are also plotted as solid triangles.

Figure 2: [below] Maximum principal stress assumed in this study. Its directions (cave bars) are shown along the fault (bold lines). In the southern part, it directs to N40°E, whereas it is to N17°E at the northern part. The numbers along the fault are grid numbers (#) used in the calculation. Main fault extends from #1 to #99, the branching points exist at #22, 31, 48, 54, 65 and 68, and the hypocenter (star) is located at #11 ($\Delta s = 0.75$ km).
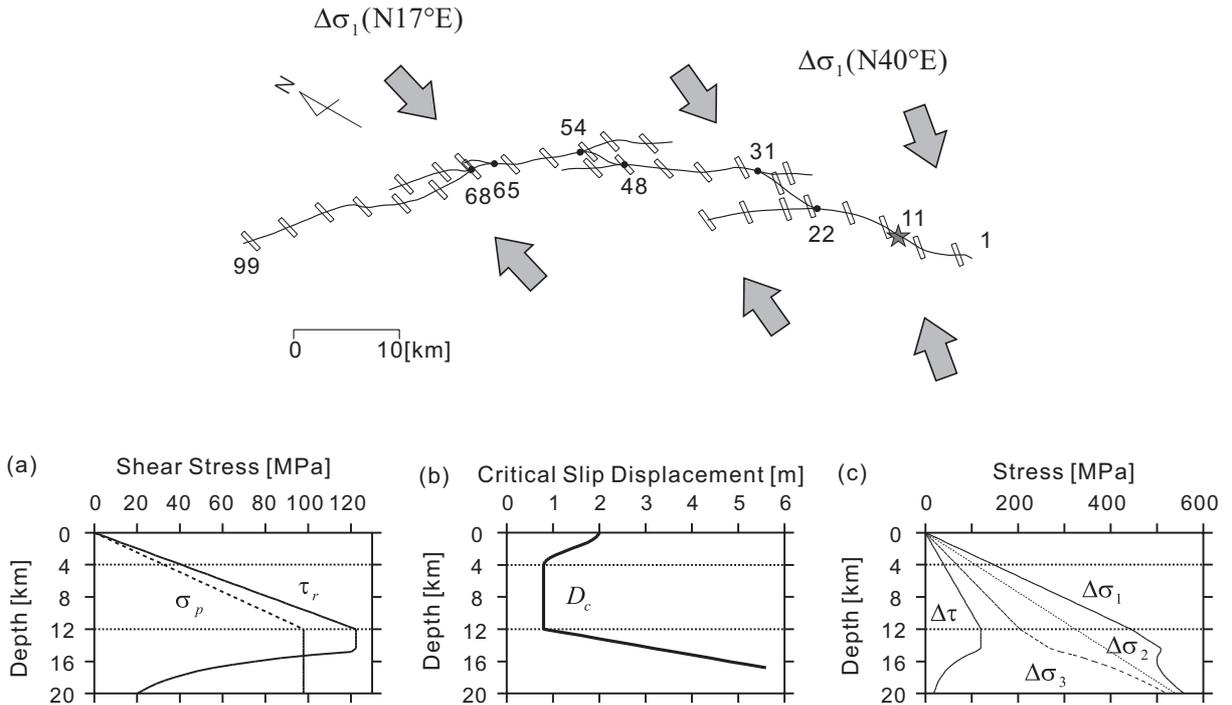

Figure 3: Depth dependence of constitutive parameters and external forces supposed in this study. (a) Peak strength σ_p and residual stress level τ_r, (b) critical slip displacement D_c, and (c) magnitude of principal stress $\Delta\sigma_1$, $\Delta\sigma_2$ and $\Delta\sigma_3$ and the induced maximum shear stress $(\Delta\sigma_1 - \Delta\sigma_3)/2$.

stress field along the fault system. Figure 2 shows the fault geometry and the direction of the maximum principal stress axis $\Delta\sigma_1$. It was assumed to rotate counterclockwise as northward, and the intermediate principal stress axis $\Delta\sigma_2$ was supposed to be vertical. Finally we introduce a slip-dependent law based on Ida (1972) [6], Sibson (1982)[13], Scholz (1988)[12], Ohnaka (1992)[8], Yamashita and Ohnaka (1992) [17], Ide and Takeo (1997)[7] and so on. Its
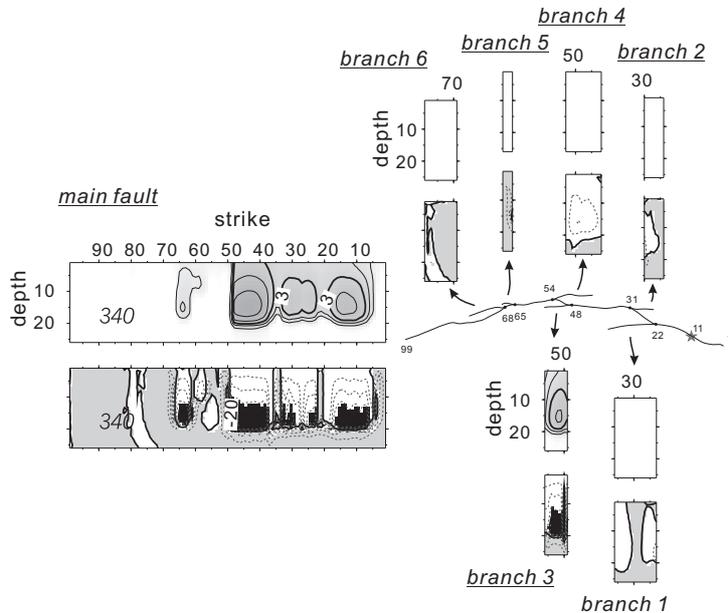
Figure 4: Final state of the simulation at time step 340 (about 23 seconds after). Top and bottom rows represent slip distribution and shear stress change, respectively. Contours are at the interval of 1 m and 5 MPa, respectively. In the stress figures (bottom), the shaded area shows positive change, while the white area shows stress release. We can see that the stress was released on the branch where the fault did not rupture (branch 1, for example).

mathematical expression was written as

$$\tau(\Delta u) = \tau_r + (\sigma_p - \tau_r)(1 - \Delta u/D_c)H(1 - \Delta u/D_c). \qquad (1)$$

Fault strength (τ) is a function of slip displacement (Δu). Here σ_p, τ_r and D_c are peak strength, residual stress level, and critical slip displacement, respectively, and $H(\cdot)$ is a Heaviside function. Figure 3(a,b) shows the depth dependence of those parameters, and the magnitude of principal stress ($\Delta\sigma_1$, $\Delta\sigma_2$ and $\Delta\sigma_3$) is illustrated in Figure 3(c). $\Delta\tau(\equiv (\Delta\sigma_1 - \Delta\sigma_3)/2)$ in the figure also represents the maximum shear stress on the plane inclined 45° from the $\Delta\sigma_1$ direction. We did not introduce any horizontal heterogeneity on the frictional parameters such as any artificial asperities in the following example.

Discussion

Figure 4 is the total slip distribution and the stress change at the final step in the simulation. We observed that the rupture does not propagate on the branch 1 (northern Johnson Valley fault), but it transferred to the northern end along the main fault (Figure 4). The key factor to reproduce it was the rotation of principal stress axis $\Delta\sigma_1$ and the non-planar fault structure. As long as we see the horizontal slip distribution, it was similar to the observation that the large slip areas appeared four times, especially at the northern part of Homestead Valley fault (around grid #45), although the slip on the last segment (Camp Rock fault) was rather small. Total seismic moment released in this simulation was estimated about 9×10^{19} Newton-meters, and it is consistent with other seismic analysis (e.g. Wald and Heaton, 1994[16]).

In all cases, large slip appeared around the depth of 13 km in the simulation, since the stress drop ($\tau_0 - \tau_r$), the difference between initial shear stress and residual stress level, and the breakdown strength drop $\Delta\tau_b(\equiv \sigma_p - \tau_r)$ were supposed to be the maximum as shown in Figure 3. That is why the model could not reproduce the character of surface slip distribution. In the field, the fault slip sometimes reaches 4 or 5 m, and the maximum slip was obtained at the surface (Hart *et al.* [5]; Wald and Heaton (1994)[16]). It is clear that a simple depth dependent frictional parameters assumed in Figure 3 is not sufficient any more. For the purpose to explain the observed surface slip distribution, we have to reform the
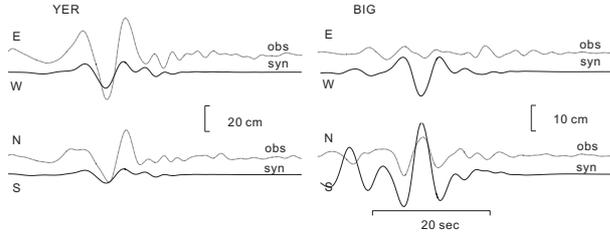
3

Figure 5: Comparison between observed ground motion (thin) and synthetic one (thick) obtained from the model. Station names are illustrated in Figure 1. Seismograms are bandpass filtered between 0.07 and 0.5Hz.

friction law so as to have finite stress drop at the shallow crust and/or introduce heterogeneity both horizontally and vertically so that stress can accumulate at that region. Olsen *et al.* (1997)[9] and Peyrat *et al.* (2000)[10] assumed the uniform frictional properties for a planar fault model, in which the breakdown strength drop $\Delta\tau_b$ was about 12 MPa at the surface and the assumed initial stress was very heterogeneous vertically as well as horizontally. The analysis by Bouchon *et al.* (1998)[3] also showed strong heterogeneity of initial stress on the fault. For further progress, we have to distinguish the universal properties of frictional parameter corresponding to Figure 3 from the intrinsic heterogeneity of fault properties. The latter subject might be more difficult to elucidate, and require not only to investigate the past seismicity around the fault system and the other seismological and geological information but also to construct any theoretical model to interpret them.

As the next step of this study, it is possible to calculate synthetic seismograms based on the rupture history of our model as shown in Figure 5. We will show some preliminary results calculated from the above simulation result. Since the station YER is located in the forward direction of rupture propagation (Figure 2), the seismogram must be affected by the rupture process itself. Although we observed the similar phases both in observational and synthetic seismograms, those amplitude in synthetic were small. That could be due to the discrepancy of the slip distribution in the shallow portion, especially on the northern segment (Camp Rock fault) close to the station, as discussed above. On the other hand, at the other station BIG which is located westward of the hypocenter, synthetic amplitude was rather large. We considered that it was caused by the procedure in which we initiated rupture around the hypocenter compulsively and which also produced a large slip area around #11 in Figure 4. Around the hypocenter, the stress might have been already released before the earthquake. Exactly speaking, we need to begin with the quasi-static simulation producing a critical initial crack. For the rest stations, we could not yet obtained the characteristic features between synthetic and observational seismograms. After refining the rupture model, we should discuss them again.

Summary

We scrutinized the fault model of the 1992 Landers earthquake (Aochi and Fukuyama, 2000). The former model did not seem to be minute enough to discuss the quantitative feature of this earthquake yet. We considered that was caused mainly by the uncertainty of vertical and horizontal distribution of frictional parameters. A simple model shown in Figure 3 was not always sufficient if one wants to look in more detail. Any kinds of heterogeneity which cannot be described must exist on the fault whatever friction law we suppose. In any case, absolute evaluation of frictional parameters (σ_p and τ_r) must be necessary as well as its qualitative change ($\Delta\tau_b$) for understanding the rupture physics along non-planar faults. At the same time, we have to make clear the field information such as the lateral variation of stress. For further works, we will have to compare the simulation with the others (e.g. Peyrat *et al.*, 2000[10]) in different setting (one planar fault in 3D vertically layered medium) with different

method (finite difference method) by assuming the same initial situation, because the single planar fault model might include both intrinsic heterogeneity of fault properties and that apparently produced by the approximation of the non-planar fault structure.

Acknowledgments

References

[1] Aki, K., and Richards, P. G., 1980, *Quantitative Seismology: Theory and Methods,* Freeman and Co., San Francisco.

[2] Bonnet, M., 1995, *Boundary Integral Equation Methods for Solids and Fluids,* John Wiley & Sons Ltd, Chichester, England.

[3] Bouchon, M., M. Campillo and F. Cotton, 1998, *Stress field associated with the rupture of the 1992 Landers, California, earthquake and its implications concerning the fault strength at the onset of the earthquake,* J. Geophys. Res., **103**, 21091-21097.

[4] Dokka, R. K. and C. J. Travis, 1990, *Late Cenozoic strike-slip faulting in the Mojave Desert, California,* Tectonics, **9**, 311-340.

[5] Hart, E. W., W. A. Bryant and J. A. Treiman, 1993, *Surface Faulting Associated with the June 1992 Landers Earthquake, California,* Calif. Geol., **46**, 10-16.

[6] Ida, Y., 1972, *Cohesive Force across the Tip of a Longitudinal-Shear Crack and Griffith's Specific Surface Energy,* J. Geophys. Res., **77**, 3796-3805.

[7] Ide, S., and M. Takeo, 1997, *Determination of constitutive relations of fault slip based on seismic wave analysis,* J. Geophys. Res., **102**. 27379-27391.

[8] Ohnaka, M., 1992, *Earthquake source nucleation: a physical model for short term precursors,* Tectonophysics, **211**, 149-178.

[9] Olsen, K. B., R. Madariaga and R. J. Archuleta, 1997, *Three-Dimensional Dynamic Simulation of the 1992 Landers Earthquake,* Science, **278**, 834-838.

[10] Peyrat, S., K. Olsen and R. Madariaga, 2000, *Dynamic Modeling of the 1992 Landers Earthquake,* submitted to J. Geophys. Res.

[11] Quin, H., 1990, *Dynamic stress drop and rupture dynamics of the October 15, 1979 Imperial Valley, California, earthquake,* Tectonophysics, **175**, 93-117.

[12] Scholz, C. H., 1988, *The brittle-plastic transition and the depth of seismic faulting,* Geol. Rund., **77**, 319-328.

[13] Sibson, R. H., 1982, *Fault zone models, heat flow, and the depth distribution of earthquakes in the continental crust of the united states,* Bull. Seism. Soc. Am., **72**, 151-163.

[14] Sowers, J. M., J. R. Unruh, W. R. Lettis and T. D. Rubin, 1994, *Relationship of the Kickapoo Fault to the Johnson Valley and Homestead Valley Faults, San Bernardino Country, California,* Bull. Seism. Soc. Am., **84**, 528-536.

[15] Unruh, J. R., W. R. Lettis and J. M. Sowers, 1994, *Kinematic Interpretation of the 1992 Landers Earthquake,* Bull. Seism. Soc. Am., **84**, 537-546.

[16] Wald, D. J. and T. H. Heaton, 1994, *Spatial and Temporal Distribution of Slip for the 1992 Landers, California, Earthquake,* Bull. Seism. Soc. Am., **84**, 668-691.

[17] Yamashita, T. and M. Ohnaka, 1992, *Precursory surface deformation expected from a strike-slip fault model into which rheological properties of the lithosphere are incorporated,* Tectonophysics, **211**, 179-199.